Quantum choice models leap out of the laboratory: capturing real-world behavioural change.

Thomas O. Hancock, Charisma F. Choudhury[1], Joan Walker[2], and Stephane Hess[1]

[1]Choice Modelling Centre and Institute for Transport Studies, University of Leeds, UK
[2]Civil and Environmental Engineering, University of California, Berkeley, USA

Short summary

Quantum choice models have been recently introduced to travel behaviour modelling, showing significant promise in explaining preferential change as a result of a change in choice context. However, thus far, quantum choice models have only been applied to stated preference (SP) data. This paper focusses on the application of these models to revealed preference (RP) data and the methodological adaptations required to deal with the increased complexities that come with RP data. Using 2-week travel diaries from 273 individuals in/near Leeds, UK, we demonstrate that quantum choice models can effectively capture the impact of behavioural nudges used to shift travellers towards greener travel modes. The results demonstrate that the provision of feedback on behaviour relative to those of a similar demographic reinforces current behaviour: travellers who make more green choices become greener, whilst the converse is true for travellers who use make less green choices than average.
Keywords: Behavioural change; Quantum choice model; Quantum rotations; Revealed preference data.

1 Introduction

Quantum probability, first developed in theoretical physics, has recently made the transition into cognitive psychology, where it has been used to explain the impact of question order, fallacies in decision-making, and other effects that were previously difficult to explain using classical models (Pothos & Busemeyer, 2022). In our previous work, we demonstrated that quantum probability theory could also make the transition into choice modelling through the development of quantum choice models, and be used to explain route choice behaviour (Hancock et al., 2020b) as well as moral choice behaviour (Hancock et al., 2020a). In particular, the results revealed that the quantum choice models can efficiently capture the effect of a change in choice context through 'quantum rotations' in stated preference choice settings.

However, the applicability of the methods in real-world settings, where the context effects are more 'fuzzy' and difficult to capture in the data, remains unclear. Furthermore, the model has not previously been applied to datasets where there are different numbers of alternatives in different choice contexts, nor has it been applied to choice contexts where there are different numbers of attributes for different alternatives.

In this paper, we aim to address these research gaps by testing quantum choice models on revealed preference (RP) data from a natural experiment involving behavioural interventions/nudges potentially leading to shifts in the choice context. We aim to test whether quantum choice models better capture behavioural changes arising from interventions and whether they lead to similar or different behavioural insights in comparison to typical modelling approaches.

The remainder of this paper is arranged as follows. First, the current and standard implementations of quantum choice models are described, before new theories and extensions for the model are detailed. Next, we discuss a real-world case study of mode choice with nudge interventions in the UK, before presenting conclusions and possibilities for future research.

2 Methodology

First we present an overview of quantum concepts. Next, we outline the 'quantum amplitude model', specifying different levels of model complexity. Finally, we demonstrate how the model

captures a change in choice context.

Overview of the quantum concepts

As is the case for any choice model, a quantum choice model captures the quality of each alternative and produces a set of probabilities for the likelihood of choosing each alternative. The representation of the alternatives, however, is very different to that of standard econometric choice models. Under quantum choice models, a series of choices (i.e. where, how and when to travel) is represented by a 'Hilbert space', H. This space is similar to Euclidean space, except that it uses complex numbers and is of dimension J, where J represents the number of alternatives. Each individual choice (where, how and when) is itself represented by a subspace, L, within the Hilbert space. Each subspace, L, is created by a basis of vectors (e.g. $|x_1\rangle, |x_2\rangle, ..$) where each vector represents an alternative and has real and imaginary parts. In line with previous notation used in quantum cognition, we use 'bra-ket' notation (Trueblood & Busemeyer, 2011), under which a column vector in a Hilbert space is represented by a 'ket' vector, $|\cdot\rangle$, with the corresponding row vector (with each element being complex conjugated) a 'bra' vector, $\langle\cdot|$. A representation of a subspace is given in Figure 1.

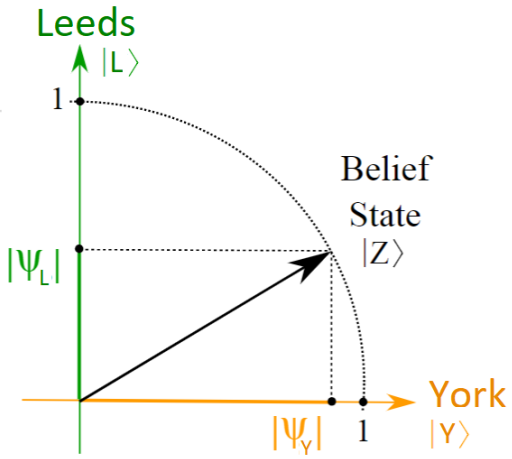

Figure 1: An example of a subspace representing a destination choice, where the individual can choose to travel to Leeds or York (adapted from Hancock et al. 2020b). Leeds is represented by the vector $|L\rangle$ and York is represented by $|Y\rangle$, with the decision-maker's current preference represented by $|Z\rangle$.

The preferences of the individual (e.g. to choose to travel to York or Leeds in Figure 1) are contained within a 'state' vector, $|Z\rangle$, which is a superposition of the alternative vectors and represents the decision-maker's propensity to choose different alternatives. By 'choosing' an alternative, the decision-maker's 'state' vector aligns with the vector representing the chosen alternative through a projection from the state vector. This results in the possibility of complex interactions between pairs of choices (e.g. where and how) as the choice of an alternative for where can impact the probability of choosing different alternatives for how (e.g. a shopper who wishes to travel by car may choose to travel to a place with better parking facilities). A visualisation of this is provided in Figure 2.
The shift in probability is a direct result of the decision being made from a different state. In the example provided in Figure 2, the projection length for Leeds, $||\psi_L\rangle|$, is increased if the decision-maker chooses their destination from $|T\rangle$ instead of $|Z\rangle$.

The quantum amplitude model (QAM)

The quantum amplitude model (QAM, Hancock et al. 2020b) defines probabilities for alternatives based on the use of projection lengths for each alternative, $||\psi_i\rangle|$. As the state vector representing the decision-maker's preferences is normalised to be of unit length and the vectors for the different alternatives are orthonormal, the probability for choosing the alternative can be set to its squared projection length. In Euclidean space, this is a direct result of the use of Pytagoras' Theorem, see

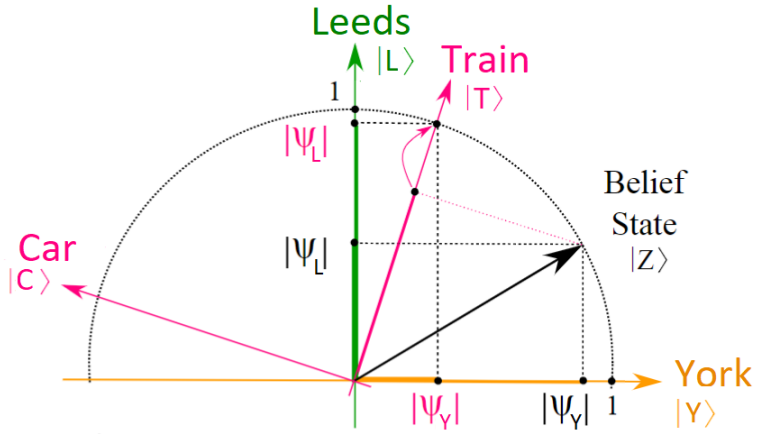

Figure 2: An example of a pair of choices. The choice of either travelling by car or train impacts the probability of choosing to travel to York or Leeds.

Figure 1. In Hilbert space, the use of complex conjugates (Hancock et al., 2020b) ensures that this property holds. Thus, we have:

$$P(j) = |\psi_j|^2 = \psi_j \cdot Conj(\psi_j), \tag{1}$$

where $|\psi_j|$ is the norm of the 'amplitude' and we have:

$$\sum_{j}^{J} |\psi_j|^2 = 1. \tag{2}$$

Consequently, we can build a quantum choice model simply by defining a normalised state vector, which, like a standard econometric choice model, can be based on the attributes of the alternatives. The state vector components (with respect to each alternative vector) can be based on utility function differences (e.g. regret functions (Chorus, 2010) work particularly well, Hancock et al. 2020b), as this results in larger projection lengths for alternatives with favourable attributes, which increases the probability of these alternatives being chosen. Thus, under our most basic specification for a quantum choice model, for alternative i, for individual n in choice task t, we define:

$$|\psi_{int}| = \delta_i + \sum_{k=1}^{K} \sum_{j \neq i}^{J} (A_{i,j} \cdot ln(1 + e^{\beta_k (x_{intk} - x_{jntk})})) \tag{3}$$

where δ_i is equivalent to alternative specific constants in econometric choice models, and captures the underlying bias towards an alternative. β_k captures the relative importance of attribute k, the elements x represent the attribute levels and $A_{i,j}$ is an indicator variable taking the value of 1 if alternatives i and j are both available in the current choice context.
In the work using quantum choice models thus far, the number of possible alternatives has always been constant across the dataset. This is not necessarily the case in RP data, where, for example, car availability will impact the number of possible alternatives. As regret functions are used, a correction may be required (Van Cranenburgh et al., 2015). Thus, the second QAM model is defined using average differences through the use of J_{nt}, the number of available alternatives for individual n in choice task t:

$$|\psi_{int}| = \delta_i + \sum_{k=1}^{K} \sum_{j \neq i}^{J} (A_{i,j} \cdot ln(1 + e^{\beta_k (x_{intk} - x_{jntk})}))/(J_{nt} - 1). \tag{4}$$

To properly exploit the fact that the quantum choice model can operate in complex space (with real and imaginary parts), our third version of the model incorporates 'complex phases', $e^{i \cdot \theta_k}$, to introduce imaginary parts to the amplitudes. This aims to capture the fact that different attributes may not be considered equivalently during the choice deliberation process (Hancock et al., 2020a). Thus we have:

$$|\psi_{int}| = \delta_i + \sum_{k=1}^{K}\sum_{j\neq i}^{J}(e^{\mathrm{i}\cdot\theta_k}\cdot A_{i,j}\cdot ln(1+e^{\beta_k(x_{intk}-x_{jntk})}))/(J_{nt}-1). \tag{5}$$

Finally, further flexibility can be introduced by introducing complex phase multipliers ($e^{\mathrm{i}\cdot\theta_i}$) to the alternative specific constants:

$$|\psi_{int}| = \delta_i\cdot e^{\mathrm{i}\cdot\theta_i} + \sum_{k=1}^{K}\sum_{j\neq i}^{J}(e^{\mathrm{i}\cdot\theta_k}\cdot A_{i,j}\cdot ln(1+e^{\beta_k(x_{intk}-x_{jntk})}))/(J_{nt}-1), \tag{6}$$

where the phase for one alternative is fixed to ensure identification.

Capturing a change of choice context

Under quantum choice models, the impact of a nudge can be captured by a 'quantum rotation,' which shifts the state vector. Preferences for two separate tasks/actions are represented by the same state vector (i.e. we would have the same state vector representing preferences/the propensity to choose which mode to travel, and where an individual chooses to travel, see Figure 1). Vectors representing alternatives in the first task are not the same as vectors representing alternatives in the second, but are not necessarily orthonormal across tasks, meaning that making one decision (and thus 'projecting' onto the vector represented by the first chosen alternative), will shift the decision-maker's state vector, but ultimately mean that they can still choose any of the alternatives in the second task. Consequently, the probabilities of choosing the different alternatives in the second task may change (i.e. trying to be more environmentally friendly will reduce the likelihood of choosing to drive). This concept of 'entanglement' is the key factor in driving the improvement found by adopting quantum models within case studies on ordering effects in cognitive psychology. In the current context, behavioural nudges are represented mathematically through the use of a quantum rotation to the state vector prior to the decision-maker choosing an alternative. For example, an individual may implicitly answer the question 'Am I an environmentally friendly person?' if they are nudged towards making greener choices. The more environmentally conscious the individual, the larger the rotation and consequential shift towards greener alternatives. Mathematically, a rotation maps amplitudes onto new ones through multiplication:

$$\psi'|_j = \sum_{i=1}^{n} U^*_{j,i}\cdot|\psi_j|, \tag{7}$$

where the unitary matrix U must have certain properties to ensure that a new belief state vector maintains unit length. In the case in hand, the use of *Hamiltonians*, (H), control the change of the belief state vector according the dynamics of the Schrödinger equation:

$$U(\tau) = e^{-\mathrm{i}H\tau}, \tag{8}$$

where H itself must be Hermition to ensures that the time evolution (over τ) will conserve the normalisation of the belief state. The size of H will depend on the number of available alternatives. For two alternatives, it is defined:

$$H = \begin{bmatrix} 1 & \delta_{H_{12}} \\ Conj(\delta_{H_{12}}) & -1 \end{bmatrix}, \tag{9}$$

where $\delta_{H_{ij}}$ is a parameter to be estimated that governs the degree to which an individual's preference shifts between alternatives i and j.

3 Empirical application

Data

The dataset tested is from the 'Decisions' survey (Calastri et al., 2020). In this survey, 273 participants completed a 2-week travel diary with the use of Rmove. An average of 2.5 trips per day across respondents resulted in a total of 9,254 trips.
At the end of the first week, some participants were given feedback as to whether they use more or less CO2 and burn more or fewer calories than other participants with similar demographics.

In total, 128 participants received no feedback, 79 received feedback regarding their own travel, and 66 received feedback showing their own travel relative to those of a similar demographic. An example of the feedback received is shown in Figure 3.

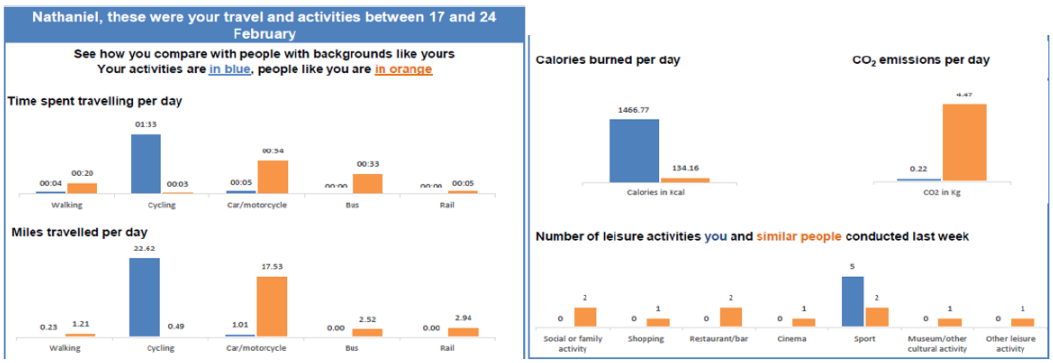

Figure 3: An example of the feedback given after one week to a participant who sees their relative performance in comparison to individuals of a similar demographic.

Corrections for correlation and endogeneity issues suggested that there was no significant impact of feedback for individuals aggregating over all their trips (Palma et al., 2019). However, analysis at the trip-level was not possible at this point as level-of-service data was only obtained for this dataset following later work (Tsoleridis et al., 2022). In the current context, quantum choice models are applied across the choice tasks with 'quantum rotations' aiming to capture the 'nudge' towards making greener choices if the individual has received feedback.

Model specification

There are up to six possible mode alternatives, listed below in Table 1. The multinomial logit model that is used for comparison is linear sum of alternative specific constants (δ), mode-specific in-vehicle travel times for non-active modes ($\beta_{mode-ivt}$), mode-specific out-of-vehicle times for active modes and public transport ($\beta_{mode-ovt}$), and costs for non-active modes (β_{cost}).

Table 1: The full set of parameters used in the base models.

	Car	Bus	Rail	Taxi	Cycle	Walk
Alternative specific constant	δ_{car}	δ_{bus}	δ_{rail}	δ_{taxi}	δ_{cycle}	δ_{walk}
In-vehicle travel time	$\beta_{car-ivt}$	$\beta_{bus-ivt}$	$\beta_{rail-ivt}$	$\beta_{taxi-ivt}$		
Out-of-vehicle travel time		$\beta_{bus-ovt}$	$\beta_{rail-ovt}$		$\beta_{cycle-ovt}$	$\beta_{walk-ovt}$
Fare/Cost	β_{cost}	β_{cost}	β_{cost}	β_{cost}		

To capture behavioural change in the MNL models, we use shifted alternative specific constants, thus we have:

$$\delta'_{i,n} = \delta_i + \delta_{co2,i} \cdot \zeta_{co2,n} + \delta_{cal,i} \cdot \zeta_{cal,n}, \tag{10}$$

where $\zeta_{co2,n} = 1$ and $\zeta_{cal,n} = 1$ if individual n has received feedback stating that they have used more CO2, and burned more calories, respectively, than individuals of a similar demographic.
For the quantum choice models, the behavioural change is incorporated through the use of Hamiltonians (see Equations 7-9). We focus on the shift towards or away from the use of car, thus have:

$$H_{car,i} = \delta_{co2,i} \cdot \zeta_{co2,n} + \delta_{cal,i} \cdot \zeta_{cal,n}, \tag{11}$$

with the other non-diagonal elements of the Hamiltonian set to a value of zero.

Results for base models

The full model results for the base MNL model and the base quantum amplitude model (QAM, based on Equation 3) are given in Table 2.
For the MNL model, we see reasonable willingness-to-pay outputs, with out-of-vehicle times generally worse than in-vehicle times, and the coefficient for walking time most negative, as would

Table 2: Model outputs and parameter estimates for the base MNL and quantum models.

Model	Base MNL			QAM (Eq. 3)		
free pars.	14			15		
LL(0)	-11,176			-11,176		
LL	**-4,057**			**-4,160**		
adj. ρ^2	0.6358			0.6265		
BIC	8,369			8,593		
par.	est	rob. t-rat	VTT (£/hr)	est	rob. t-rat	RI (£/hr)
δ_{car}	0.000	NA		36.383	3.59	
δ_{bus}	-2.908	-11.62		2.512	2.67	
δ_{rail}	-2.850	-7.30		-3.536	-2.69	
δ_{taxi}	-3.780	-10.21		3.522	3.16	
δ_{cycle}	-4.239	-9.68		-4.600	-4.23	
δ_{walk}	0.365	1.47		12.122	3.41	
$\beta_{car-ivt}$	-0.144	-9.27	41.42	-0.395	-3.31	26.93
$\beta_{bus-ivt}$	-0.049	-7.21	14.05	-0.214	-3.49	14.58
$\beta_{bus-ovt}$	-0.097	-3.28	27.81	-0.584	-4.07	39.86
$\beta_{rail-ivt}$	-0.048	-3.29	13.67	-0.157	-2.26	10.71
$\beta_{rail-ovt}$	-0.079	-5.84	22.62	-0.321	-3.53	21.88
$\beta_{taxi-ivt}$	-0.100	-3.32	28.79	-0.916	-3.55	62.50
$\beta_{cycle-ovt}$	-0.080	-5.53	22.95	-0.528	-2.96	36.03
$\beta_{walk-ovt}$	-0.154	-11.94	44.10	-0.347	-4.13	23.65
β_{cost}	-0.209	-6.71		-0.879	-3.53	

be expected. Though the quantum choice model does not produce WTP outputs, the relative importance of attributes can be estimated. These values, though within the same range as MNL WTPs, show some large discrepancies. For example, the relative importance for taxi travel time is approximately doubled, whilst it is halved for walking time.
Next, we compare model fits across the QAM models with updated specifications based on Equations 4-6. These model results are given in Table 3.

Table 3: Model fits from the different versions of quantum amplitude models

Model	MNL	QAM (Eq.3)	QAM (Eq.4)	QAM (Eq.5)	QAM (Eq.6)
Free pars.	14	15	15	17	22
LL(0)	-11,176	-11,176	-11,176	-11,176	-11,176
LL	-4,057	-4,160	-4,158	-4,059	-4,032
$adj.\rho^2$	0.6358	0.6265	0.6266	0.6353	**0.6373**
BIC	**8,369**	8,593	8,589	8,428	8,465

The inclusion of complex phases (Equation 5) results in a substantial improvement in the performance of the QAM model, bringing it in line with the result from the MNL model, though at the cost of 3 additional parameters. The addition of a further 5 complex phases results in the QAM model outperforming MNL by 25 log-likelihood units with a better adjusted ρ^2, but worse BIC.
The impact of the inclusion of the complex phases is visualised in Figure 4. If two phases overlap, this suggests 'no interference' between the two factors, meaning that the factors are fully compensatory and can be traded off against each other. Thus, in this case, as there is no interference between time and bus, this implies that there is no correlation between travel times and unobserved utility contributions towards bus. As a contrast, walk and taxi are most different.

Key differences between models

Notably, the performance of the models looks very different if they are applied to subsets of the dataset where the dataset is split based on the number of available alternatives. The model fit for choice tasks with a different number of available alternatives is given in Table 4, in which the performance of the base MNL and 4th QAM model are compared to their counterparts fitted to the subsets of data.
Most strikingly, it appears that QAM performs better than MNL for 2 or 3 alternatives, and worse for 4 or more alternatives. The QAM model also appears insufficiently adapted for datasets with differing numbers of available alternatives, with the performance of the QAM model improving more significantly than that of the MNL model when separate models are applied to subsets of data.[1]

[1]The application of correction factors (Van Cranenburgh et al., 2015), where an estimated coefficient

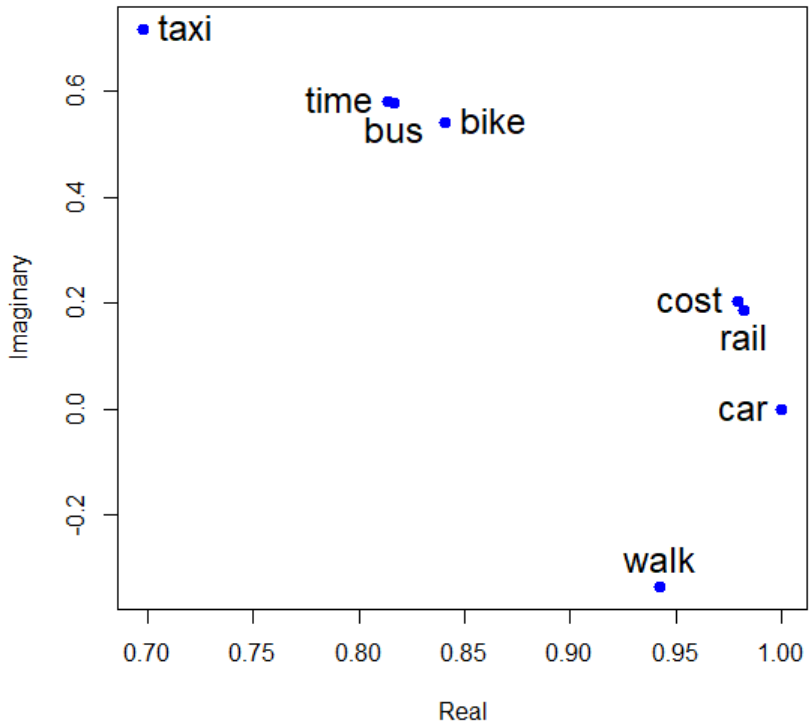

Figure 4: Inference patterns for the 4th QAM model, with the complex phase outputs for each attribute/alternative visualised in real and imaginary space.

Table 4: Contrasting performance of models applied to subsets of data based on the number of available alternatives.

		Same model			Separate models		
Available alts	Obs.	MNL	Quantum	Diff	MNL	Quantum	Diff
2 alts	1,541	-319	-317	2	-301	-281	21
3 alts	2,940	-1,473	-1,400	73	-1,434	-1,337	97
4 alts	3,630	-1,730	-1,756	-25	-1,712	-1,731	-19
5/6 alts	1,143	-534	-559	-25	-501	-511	-11
Sum	9,254	-4,057	-4,032	25	-3,948	-3,859	88

Results for models capturing behavioural change

Next, we add parameters to the MNL and QAM models to capture the shift in preference following the provision of feedback. Using Equations 10 and 11, respectively, the gain in model performance is shown in Table 5.

Positive shifts are observed for $\delta_{cal,i}$, meaning that a participant who is told they burn more calories than individuals of a similar demographic shift away from the use of a car towards the use of mode i (note that the effects for cycling and bus were insignificant and thus dropped). Negative shifts are observed for individuals who are told they burn more CO2. This implies that current behaviour is reinforced. Though results between the models appear similar, there are small differences, with the QAM in comparison to MNL suggesting a stronger relative shift for walking in comparison to rail (see Figure 5). The converse is true for the shift from taxi.

replaces $J_{nt} - 1$ in Equation 4, results in some improvement (-4,021) though not yet getting close to the gain obtained through the use of separate models (-3,859).

Table 5: Model results after the inclusion of parameters to capture behavioural change.

Model	MNL		QAM	
Base model LL	-4,056.53		-4,031.54	
LL	-4,029.68		-4,009.35	
Difference	26.85		22.20	
Extra pars.	6		6	
Likelihood Ratio Test	8.48E-10		6.214E-08	
par.	est	rob. t-rat	est	rob. t-rat
$\delta_{co2,rail}$	-1.838	-2.01	-0.207	-2.96
$\delta_{co2,taxi}$	-1.669	-2.97	-0.136	-4.49
$\delta_{co2,walk}$	-2.514	-3.58	-0.339	-7.07
$\delta_{cal,rail}$	1.522	2.21	0.221	3.16
$\delta_{cal,taxi}$	1.379	3.39	0.124	4.27
$\delta_{cal,walk}$	1.897	3.19	0.243	6.70

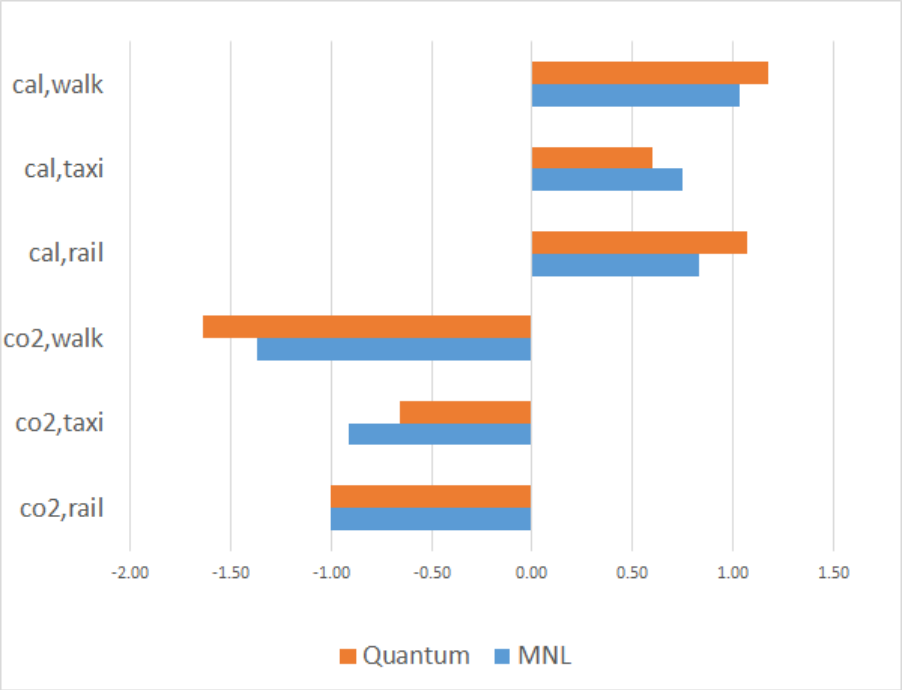

Figure 5: Relative shifts in preferences through fixing the shift from rail to car for those who used more CO2 to a value of -1 in both models.

4 Conclusions

In this work, we applied quantum choice models to revealed preference data for the first time, utilising 'quantum rotations' to capture the impact of behavioural nudges. Contrary to most examples in the literature, we find that, regardless of the modelling paradigm used, feedback reinforces behaviour, as opposed to changing behaviour. In particular, there is a shift towards choosing car if an individual is told they use more CO2 than others, whereas there is a shift away from choosing car if an individual is told that they burn more calories than others. However, these results may be subject to endogeneity biases (Palma et al., 2019), and future work should consider whether these concerns are properly accounted for in the choice models applied here.

Contrary to results from SP data (Hancock et al., 2020b,a), the base QAM model performed worse than the counterpart MNL, However, after utilisation of the full flexibility of QAM models, performance was significantly better than that of MNL, though a full interpretation of what complex phases actually capture remains a direction for future research.

Though it was not evident that QAM models are better suited than MNL models at capturing behavioural change (log-likelihood improvement was similar, see Table 5), it was clear that QAM models appear better when there are fewer available alternatives, Further work is required to establish whether these findings can be generalised.

Finally, it should be noted that extensions are possible for both models in terms of capturing heterogeneity in responses to the provision of feedback: some individuals may be more impressionable

or may simply have more opportunities to change their behaviour. Further analysis is required to better understand these possible individual differences.

Acknowledgements

Thomas Hancock and Charisma Choudhury's time were partially supported by UKRI Future Leader Fellowship [MRT020423/1]. Stephane Hess acknowledges the financial support by the European Research Council through the consolidator Grant 615596-DECISIONS.

References

Calastri, C., Crastes dit Sourd, R., & Hess, S. (2020). We want it all: experiences from a survey seeking to capture social network structures, lifetime events and short-term travel and activity planning. *Transportation*, *47*, 175–201.

Chorus, C. G. (2010). A new model of random regret minimization. *European Journal of Transport and Infrastructure Research*, *10*(2).

Hancock, T. O., Broekaert, J., Hess, S., & Choudhury, C. F. (2020a). Quantum choice models: a flexible new approach for understanding moral decision-making. *Journal of choice modelling*, *37*, 100235.

Hancock, T. O., Broekaert, J., Hess, S., & Choudhury, C. F. (2020b). Quantum probability: A new method for modelling travel behaviour. *Transportation Research Part B: Methodological*, *139*, 165–198.

Palma, D., Crastes dit Sourd, R., Calastri, C., Hess, S., & O'Neill, V. (2019). Can information really change travel behaviour? controlling for endogeneity in modelling the effect of feedback information. *Institute for Transport Studies, University of Leeds. Working paper*.

Pothos, E. M., & Busemeyer, J. R. (2022). Quantum cognition. *Annual review of psychology*, *73*, 749–778.

Trueblood, J. S., & Busemeyer, J. R. (2011). A quantum probability account of order effects in inference. *Cognitive science*, *35*(8), 1518–1552.

Tsoleridis, P., Choudhury, C. F., & Hess, S. (2022). Deriving transport appraisal values from emerging revealed preference data. *Transportation Research Part A: Policy and Practice*, *165*, 225–245.

Van Cranenburgh, S., Prato, C. G., & Chorus, C. (2015). *Accounting for variation in choice set size in random regret minimization models.* working paper.